Supporting Information

Calcium-enriched Carbon Nanoparticles Loaded with Indocyanine Green for Near-Infrared Fluorescence Imaging-Guided Synergistic Calcium Overload, Photothermal Therapy, and Glutathione-Depletion-Enhanced Photodynamic Therapy

E Pang,[a] Xiangcao Li,[a] Shaojing Zhao,[a] Yuanyu Tang,[a] Xuejian Xing,[a] Qin Wang,[a] Ke Yang,[a] Benhua Wang,[a] Shiguang Jin,[b] Xiangzhi Song,[a] and Minhuan Lan[,a]*

[a.]Hunan Provincial Key Laboratory of Micro & Nano Materials Interface Science, College of Chemistry and Chemical Engineering, Central South University, Changsha, Hunan, 410083, P. R. China.
E-mail: minhuanlan@csu.edu.cn

[b.]Center for Translational Medicine, The Affiliated Taizhou People's Hospital of Nanjing Medical University, Taizhou School of Clinical Medicine, Nanjing Medical University, Taizhou, Jiangsu, 225300, P. R. China.

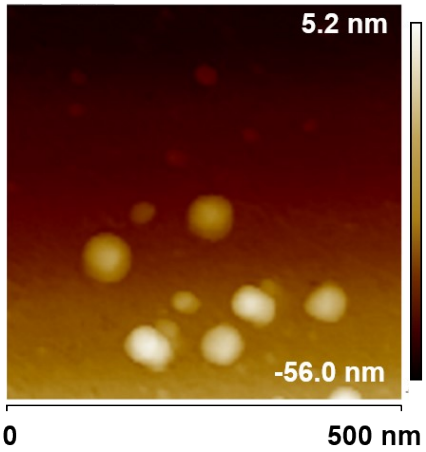

Figure S1 AFM image of Ca-CNPs.

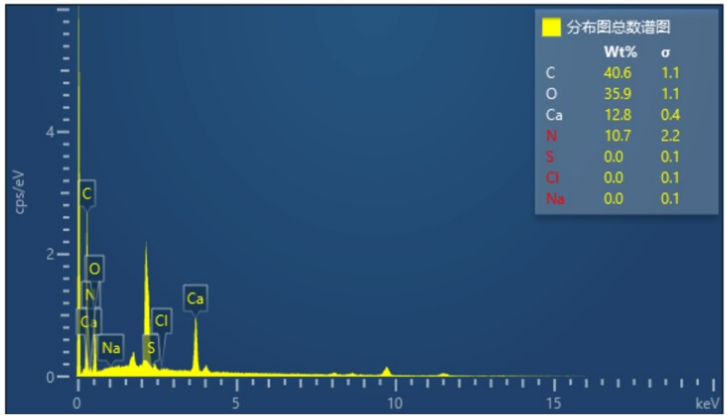

Figure S2 EDS analysis results of Ca-CNPs.

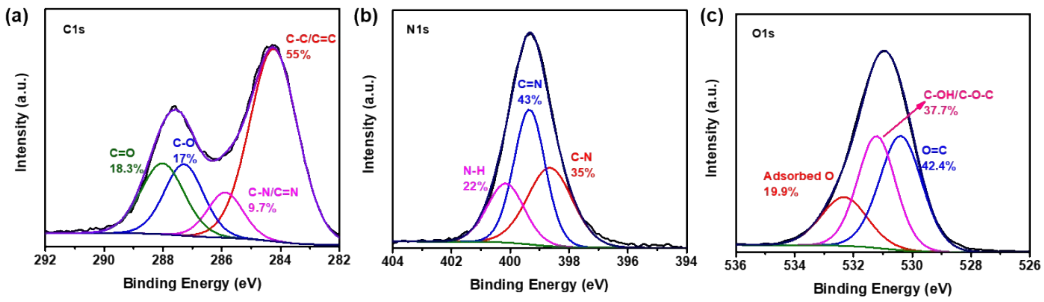

Figure S3 The deconvoluted high-resolution (a) C1s (C=O: 18.3%, C-O: 17%, C-N/C=N: 9.7%, C-C/C=N: 55%), (b) N1s (N-H: 22%, C=N: 43%, C-N: 35%) and (c) O1s (Adsorbed-O: 19.9%, C-OH/C-O-C: 37.7%, O=C: 42.4%) XPS spectra of Ca-CNPs.

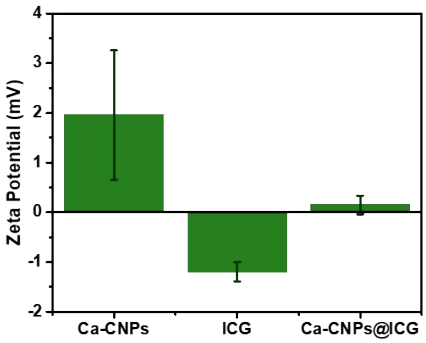

Figure S4 Zeta potential diagram of Ca-CNPs, ICG, and Ca-CNPs@ICG.

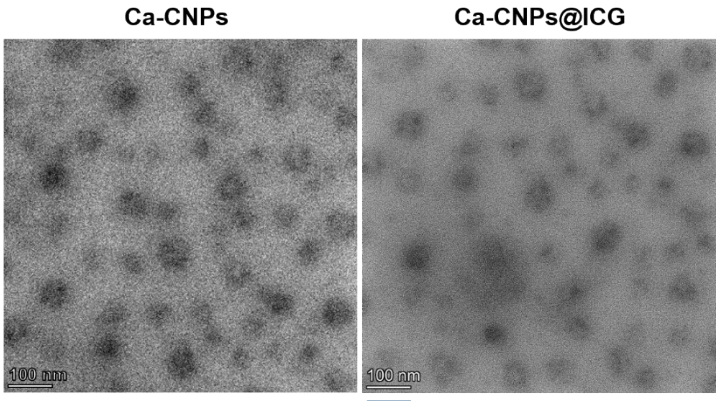

Figure S5 TEM images of Ca-CNPs (left) and Ca-CNPs@ICG (right).

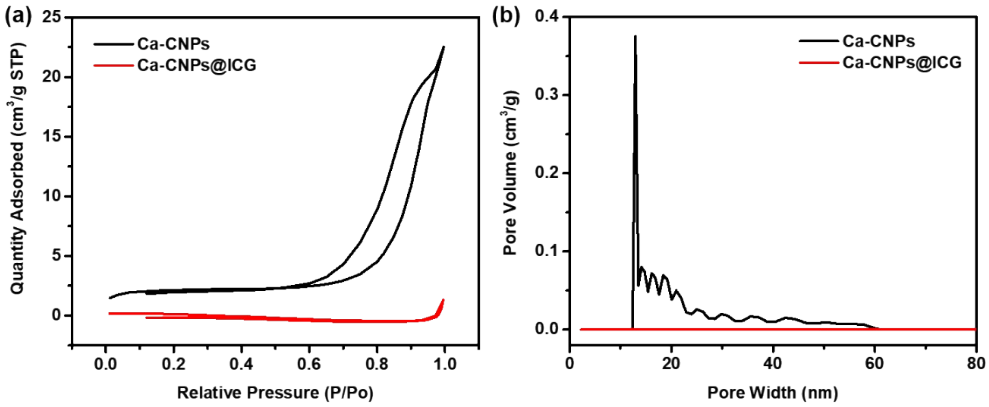

Figure S6 (a) N_2 adsorption-desorption isotherms, and (b) pore size distributions for Ca-CNPs and Ca-CNPs @ICG.

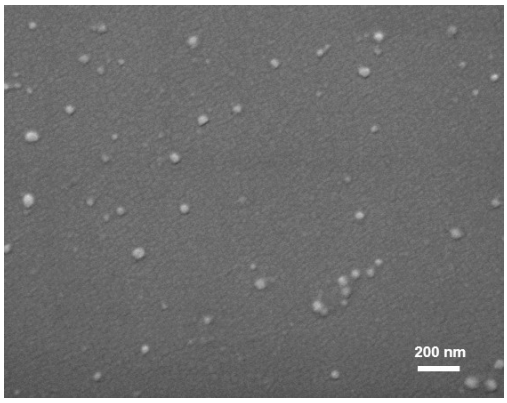

Figure S7 SEM image of Ca-CNPs@ICG aqueous solution after 6 months of preservation.

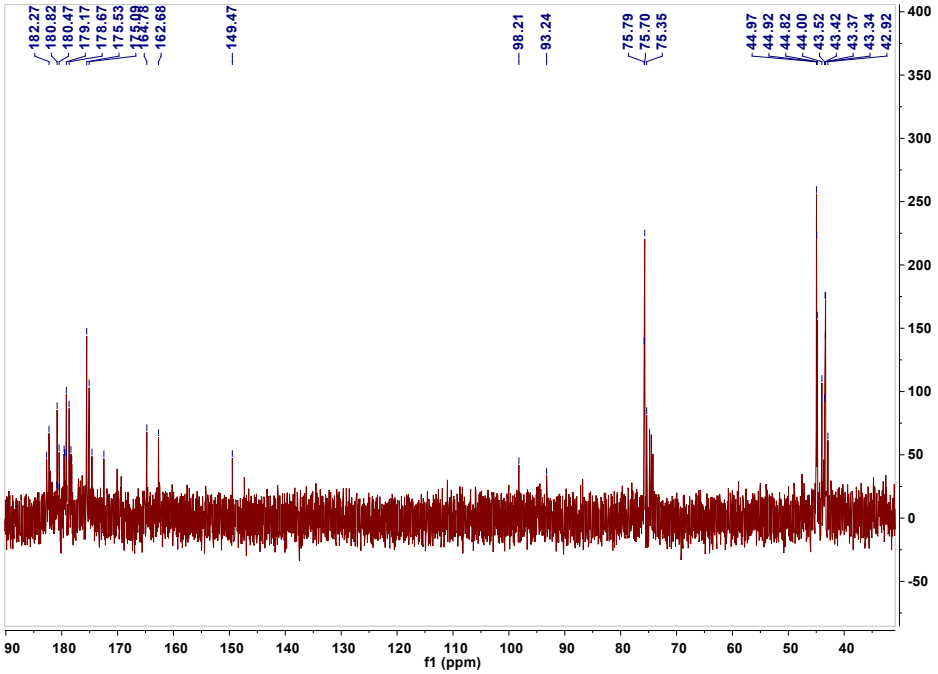

Figure S8 ^{13}C NMR spectrum of Ca-CNPs.

^{13}C NMR (400 MHz, D_2O) δ 182.70, 182.27, 180.86, 180.82, 180.47, 180.43, 180.43, 179.58, 179.49, 179.20, 179.17, 179.13, 178.67, 178.35, 178.20, 175.53, 175.09, 174.59, 172.46, 164.78, 162.68, 149.47, 98.21, 93.24, 75.79, 75.70, 75.35, 44.97, 44.92, 44.82, 44.00, 43.52, 43.42, 43.37, 43.34, 42.92.

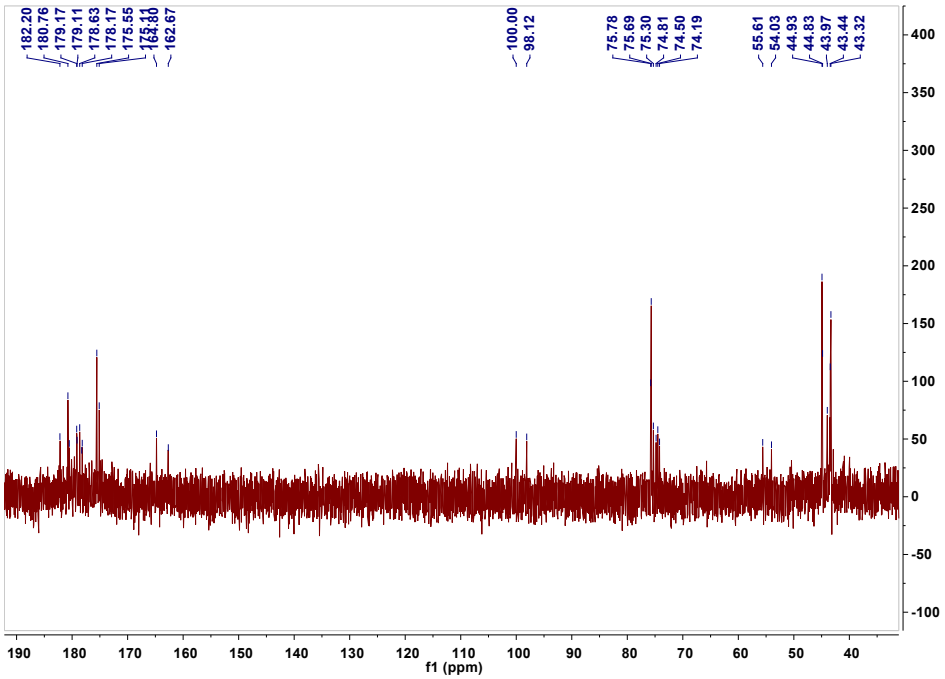

Figure S9 ^{13}C NMR spectrum of Ca-CNPs after GSH reaction.

^{13}C NMR (400 MHz, D_2O) δ 182.70, 182.27, 180.86, 180.82, 180.47, 180.43, 180.43, 179.58, 179.49, 179.20, 179.17, 179.13, 178.67, 178.35, 178.20, 175.53, 175.09, 174.59, 172.46, 164.78, 162.68, 149.47, 98.21, 93.24, 75.79, 75.70, 75.35, 44.97, 44.92, 44.82, 44.00, 43.52, 43.42, 43.37, 43.34, 42.92.

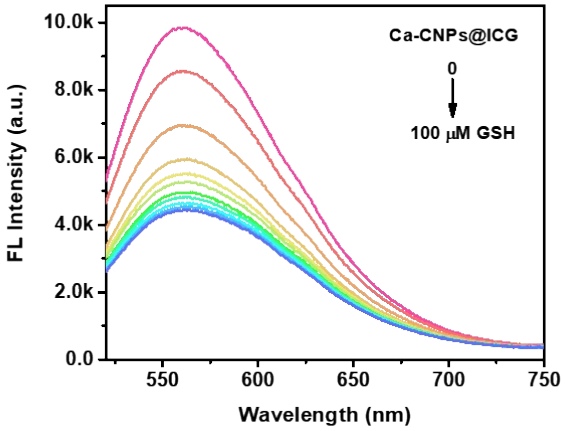

Figure S10 GSH concentration-dependent fluorescence spectra of Ca-CNPs@ICG (λ_{ex} = 490 nm).

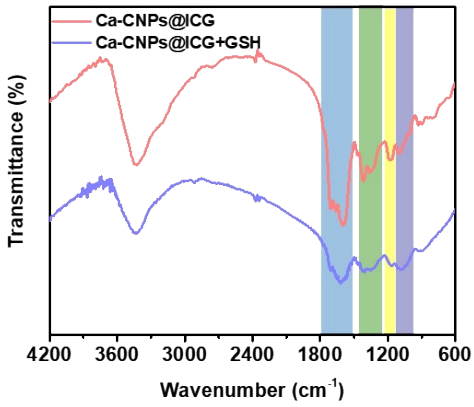

Figure S11 FTIR spectra of Ca-CNPs@ICG before and after reaction with GSH.

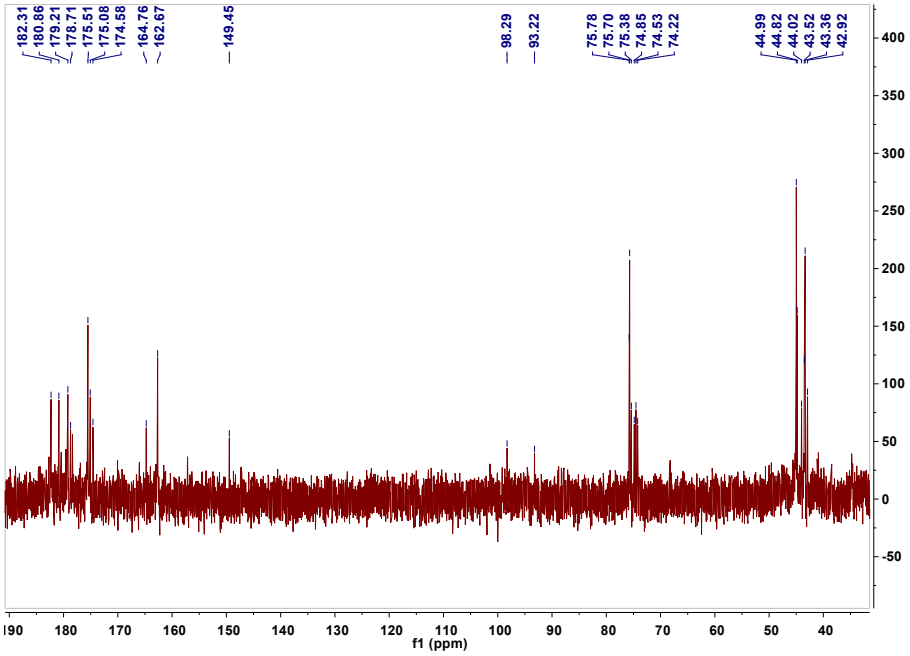

Figure S12 ^{13}C NMR spectrum of Ca-CNPs@ICG.

^{13}C NMR (400 MHz, D_2O) δ 182.70, 182.27, 180.86, 180.82, 180.47, 180.43, 180.43, 179.58, 179.49, 179.20, 179.17, 179.13, 178.67, 178.35, 178.20, 175.53, 175.09, 174.59, 172.46, 164.78, 162.68, 149.47, 98.21, 93.24, 75.79, 75.70, 75.35, 44.97, 44.92, 44.82, 44.00, 43.52, 43.42, 43.37, 43.34, 42.92.

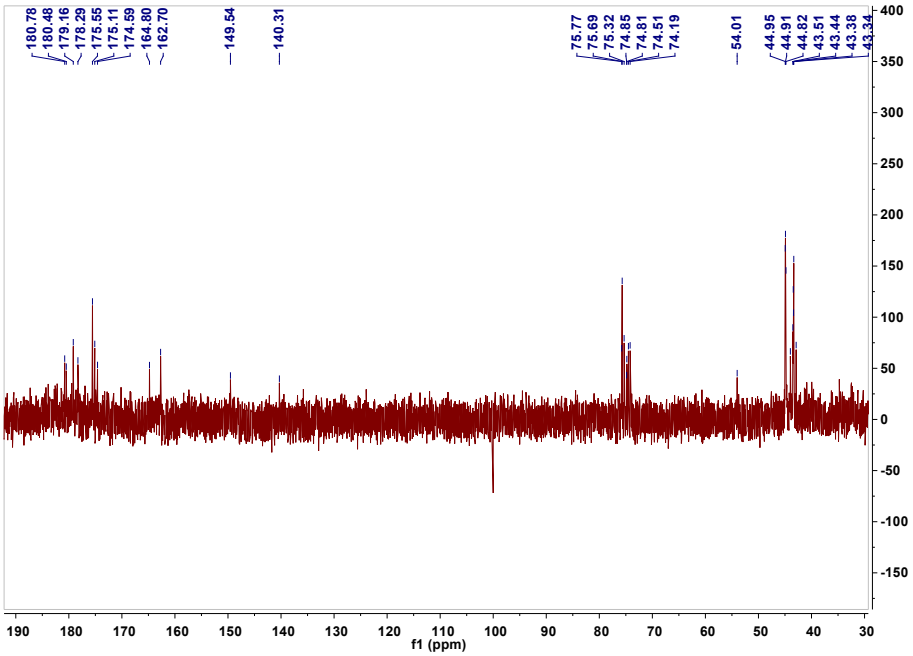

Figure S13 ^{13}C NMR spectrum of Ca-CNPs@ICG after GSH reaction.

^{13}C NMR (400 MHz, D_2O) δ 182.70, 182.27, 180.86, 180.82, 180.47, 180.43, 180.43, 179.58, 179.49, 179.20, 179.17, 179.13, 178.67, 178.35, 178.20, 175.53, 175.09, 174.59, 172.46, 164.78, 162.68, 149.47, 98.21, 93.24, 75.79, 75.70, 75.35, 44.97, 44.92, 44.82, 44.00, 43.52, 43.42, 43.37, 43.34, 42.92.

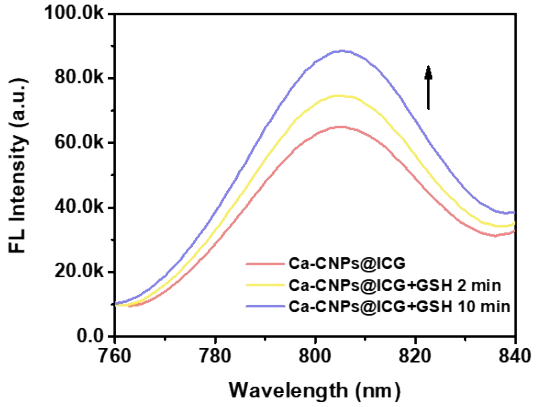

Figure S14 Time-dependent fluorescence spectra of Ca-CNPs@ICG in the presence of GSH (λ_{ex} = 750 nm).

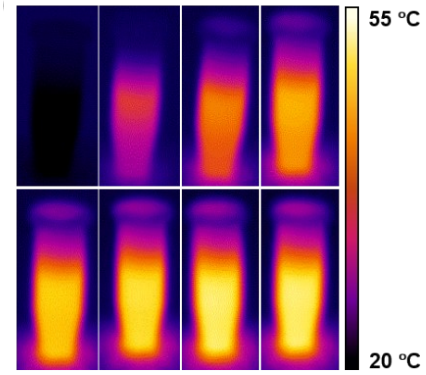

Figure S15 Time-dependent infrared thermography image of Ca-CNPs@ICG aqueous solution under 808 nm laser irradiation (1 W·cm^{-2}, 10 min).

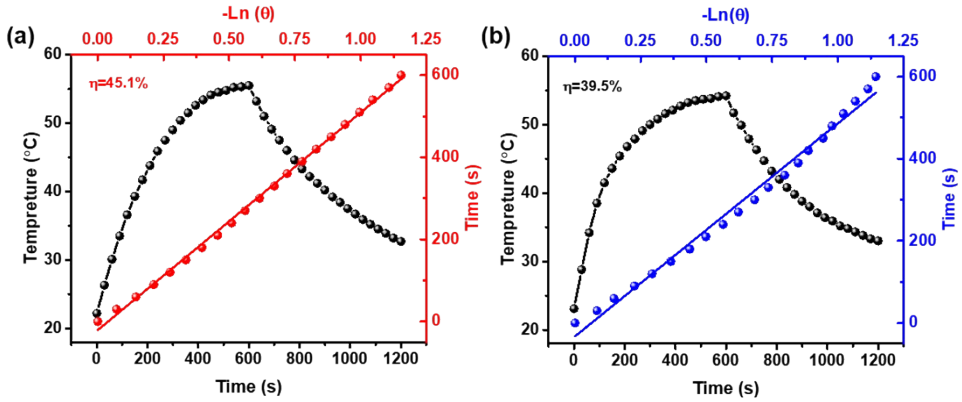

Figure S16 Temperature increasing-decreasing curve and plot of cooling time vs -Ln (θ) of (a) Ca-CNPs@ICG and (b) ICG.

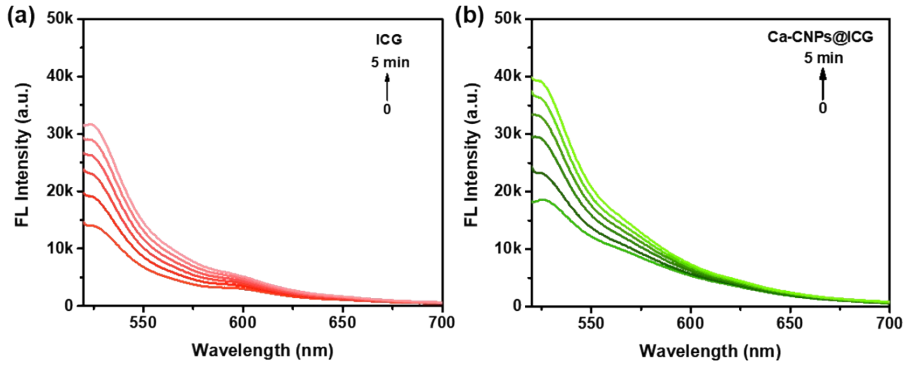

Figure S17 Time-dependent fluorescence spectra changes of SOSG mixed with (a) ICG and (b) Ca-CNPs@ICG under 808 nm laser irradiation (λ_{ex} = 504 nm, 1 W·cm^{-2}, 5 min).

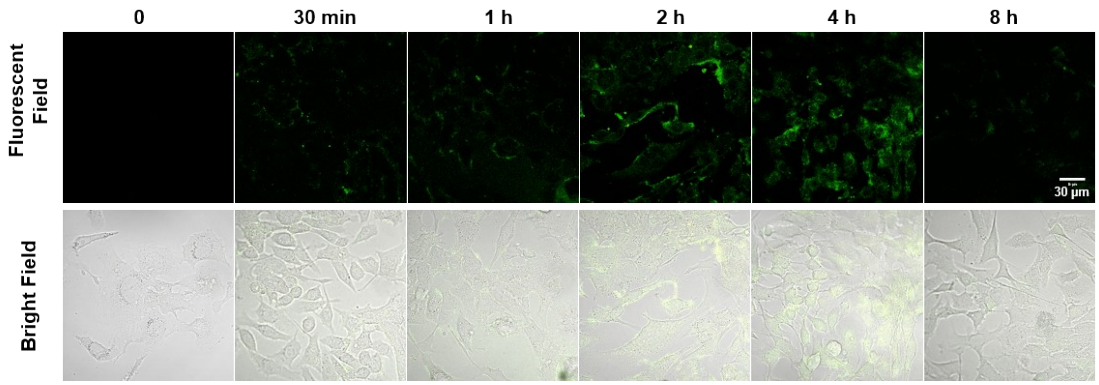

Figure S18 Cellular uptake of Ca-CNPs@ICG by 4T1 tumour cells at different moments.

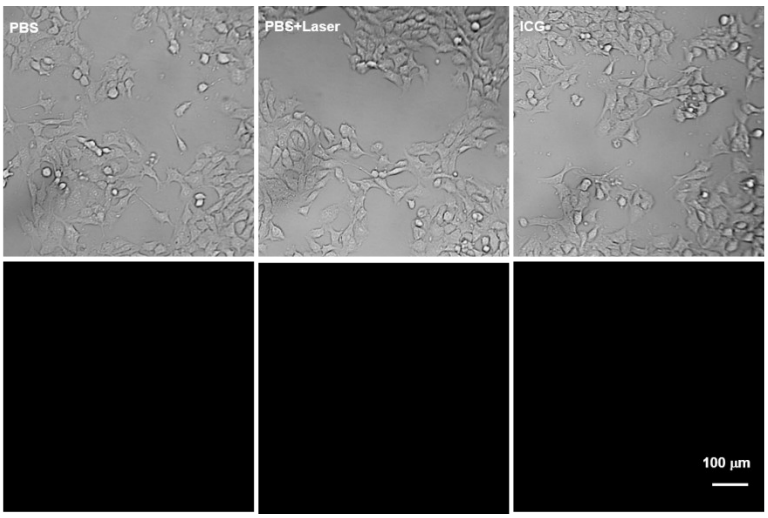

Figure S19 DCFH-DA-based fluorescence images of 4T1 cells after different treatments (808 nm, 1 W·cm^{-2}).

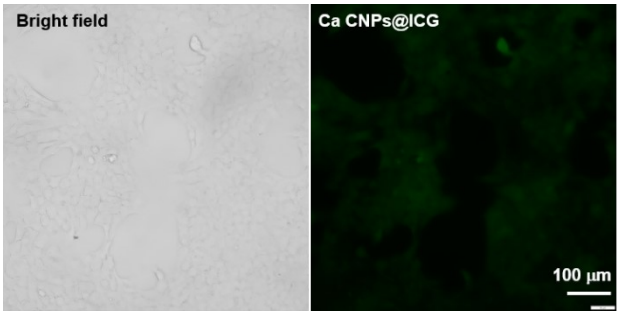

Figure S20 Fluorescence imaging of 4T1 cells after incubation with Ca-CNPs@ICG only.

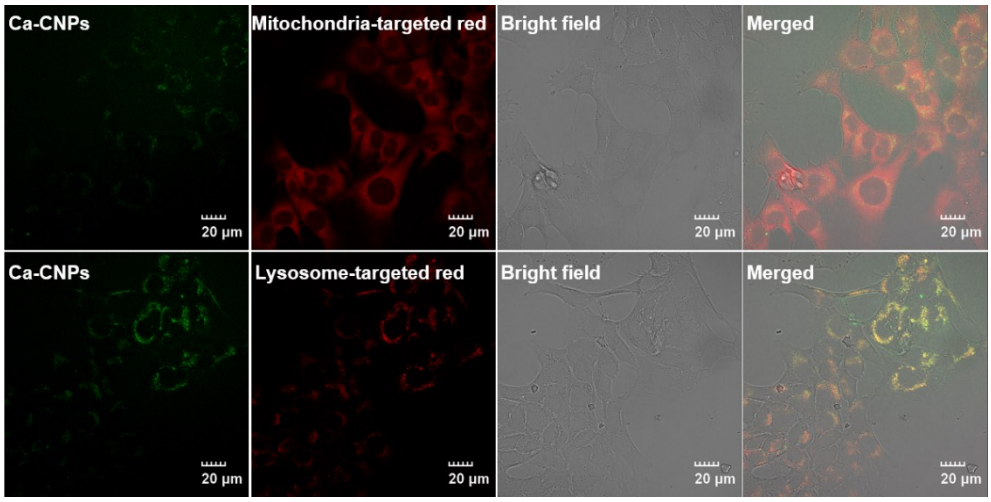

Figure S21 The confocal imaging of 4T1 cells after co-incubation of Ca-CNPs with mitochondria-targeted red or lysosome-targeted red, respectively.

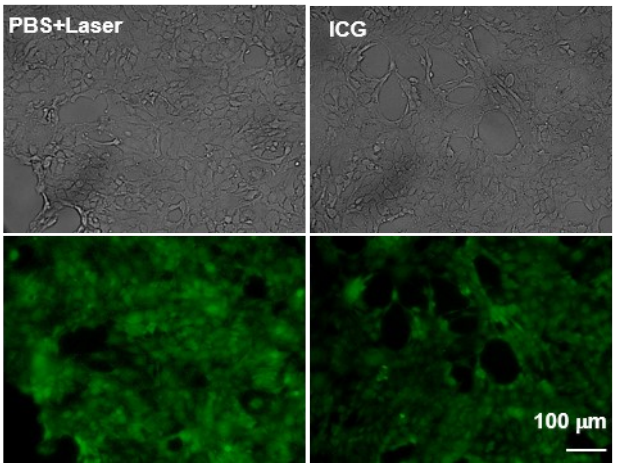

Figure S22 Calcium-AM/PI-based fluorescence images of 4T1 cells after different treatments (808 nm, 1 W·cm^{-2}).

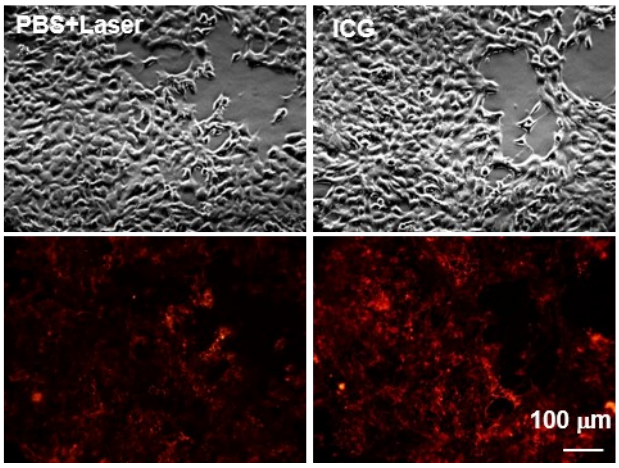

Figure S23 JC-1-based fluorescence images of 4T1 cells after different treatments (808 nm, 1 W·cm^{-2}).

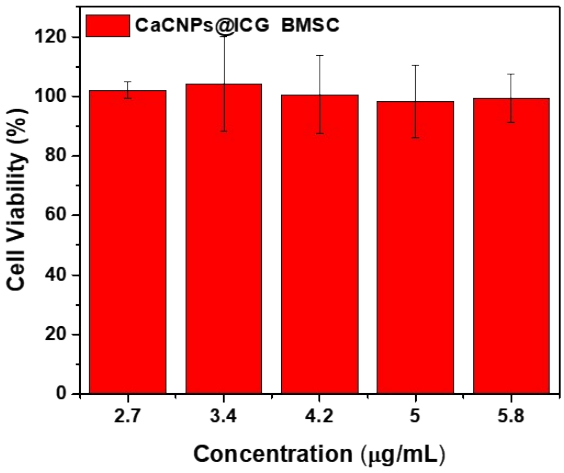

Figure S24 Cytotoxicity assay after incubation of 4T1 cells with different concentrations of Ca-CNPs@ICG.

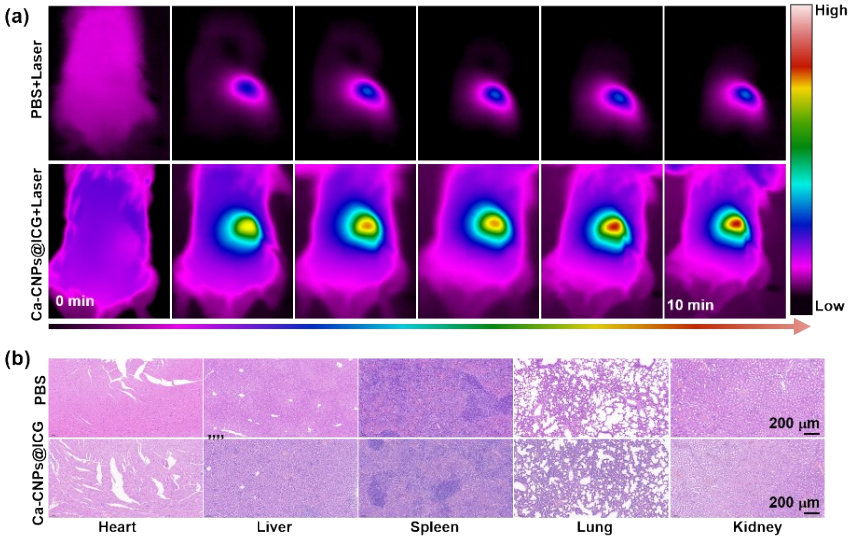

Figure S25 (a) Temperature changes at the tumour site and (b) H&E of organ sections of the mice in different treatment groups.

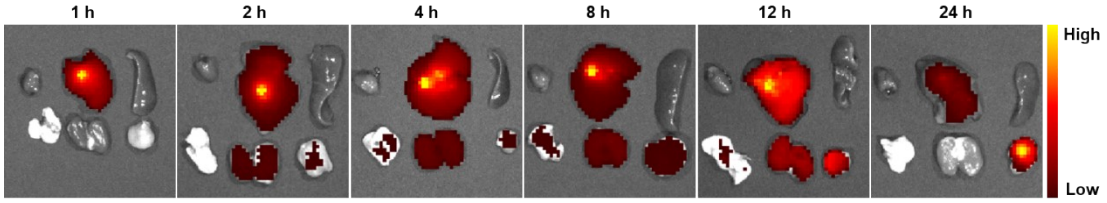

Figure S26 Fluorescence imaging of major organs of mice at different moments (λ_{ex} = 780 nm).